# Cloud-to-ground lightning activity in hail-bearing storms

Serge Soula,[1] Yann Seity,[2] Laurent Feral,[3] and Henri Sauvageot[1]

Received 7 April 2003; revised 25 September 2003; accepted 29 September 2003; published 16 January 2004.

[1] The cloud-to-ground lightning flash (CG) produced by several apparent hailstorms are analyzed in different locations of southern Europe. The hail detection is performed via four different analysis techniques: radar reflectivity factor estimation, radar echo shape analysis, polarimetric hydrometeor identification, and reflectivity difference between radars with different wavelengths. The CG parameters considered are the flash rate and density, the flash polarity, the multiplicity, and the peak current. Some of the observed storms exhibit hail-bearing cell features, while others exhibit heavy precipitation rates without any apparent hail production. One of the hailstorms can be classified as severe because reported hailstorm diameters reach 39 mm. The CG lightning characteristics of both types of storms are compared. The CG rates corresponding to all hail-bearing storms are singularly lower than those of rain-only storms, typically by a factor 5. So, the CG rate of the hail-bearing storms considered does not exceed 2 $min^{-1}$ while it can reach about 12 $min^{-1}$ for heavy rain-bearing storms. Moreover, some of them can produce especially high positive CG proportions associated with negative CGs with low values of peak current and multiplicity. This last observation suggests that the negative charge available for CG flashes is weak within the cloud when positive CG flashes are dominant. In order to interpret the low CG rates observed in the case of hail-bearing storms several interpretations are discussed, but it would be necessary to know the intracloud flash activity in such cases of storms in order to enrich the discussion. *INDEX TERMS:* 3304 Meteorology and Atmospheric Dynamics: Atmospheric electricity; 3314 Meteorology and Atmospheric Dynamics: Convective processes; 3324 Meteorology and Atmospheric Dynamics: Lightning; 3354 Meteorology and Atmospheric Dynamics: Precipitation (1854); *KEYWORDS:* lightning activity, hail, radar

**Citation:** Soula, S., Y. Seity, L. Feral, and H. Sauvageot (2004), Cloud-to-ground lightning activity in hail-bearing storms, *J. Geophys. Res.*, *109*, D02101, doi:10.1029/2003JD003669.

## 1. Introduction

[2] Few studies have reported observations about lightning activity in storms producing hail and especially large hail (diameter larger than 1.9 cm). Early research presented probabilities of occurrence of a given lightning flash rate in relation to the presence of hail in the storms. So, *Shackford* [1960] noted that no hail was observed when flash rates were less than 10 $min^{-1}$ and that the flash rates were more than 100 $min^{-1}$ in 60% of cases with hail observations. *Blevins and Marwitz* [1968] found that the probability of hail increased as the stroke rates increased up to 70 $min^{-1}$ but no hail was observed for larger stroke rates. *Baughman and Fuquay* [1970] found the flash rates higher, the flash activity period longer, and the thunderclouds taller in the thunderstorms producing hail in Montana, but they found also the flash rates were largely lower than in other regions of the United States. From a study of three hailstorms producing large hailstones, *Pakiam and Maybank* [1975] observed two cases of multicellular storms in which the hailstone sizes had a slight tendency to increase with increasing lightning rates and one case that could be a supercell with hailstones larger than 5 cm and fairly low flash rates. They suggested that low total flash rates could be a characteristic of supercells. On the contrary, from observations in the Great Plains of the United States, *Rust et al.* [1981] detected large amount of flashes associated with supercells. *Reap and MacGorman* [1989] found the probability that a storm in the Great Plains produces severe weather, increased up to 130 flashes per grid box ($48 \times 48$ $km^2$), and then decreased with still larger flash numbers.

[3] The differentiation of flash types intracloud (IC), negative cloud-to-ground (CG), and positive CG showed some particularities in hailstorms. *Reap and MacGorman* [1989] found that the probability of large hailstones considerably increased as the number of positive CG flashes increased. Several subsequent studies found severe storms whose ground flash activity consisted predominantly of positive CG flashes, and these thunderstorms often produced large hailstones during the period when they were producing positive ground flashes [*MacGorman and Burgess*, 1994; *Stolzenburg*, 1994]. The positive CG flashes usually occur during the dissipating phase of the storms [*Fuquay*, 1982],

[1]Laboratoire d'Aérologie, UMR 5560 UPS/CNRS, OMP, Toulouse, France.
[2]Météo-France, Toulouse, France.
[3]Département Electromagnétisme et Radar, Office National d'Etudes et de Recherches Aérospatiales-Centre de Toulouse, Toulouse, France.


0148-0227/04/2003JD003669

or in the stratiform region of mesoscale convective systems [*Rutledge and MacGorman*, 1988]. When they were produced in these conditions, their densities and their rates were quite low. However, some observations showed large proportions of positive CG flashes during the life of isolated storms. They could correspond to shallow cells, as indicated by *Engholm et al.* [1990] or to severe thunderstorms, as observed by *Branick and Doswell* [1992], *Seimon* [1993], *MacGorman and Burgess* [1994], *Stolzenburg* [1994], and *Carey and Rutledge* [1998]. A specific study about hail damage and CG flash rates and location was made by *Changnon* [1992]. From several cases of hailstorm which did exhibit no mesocyclones, no tornadoes, and no positive CG flashes, this study revealed that the CG locations were not colocated with hail damages. The CG rates corresponding to the Changnon study were not very large, with average values peaking at about 1–2 per minute. It is common to find larger values, for example up to 5 per minute from non-severe cases in Florida [*Holle and Maier*, 1982], or 20 per minute in negative flash-dominated severe storms [*Knapp*, 1994].

[4] Because the intracloud flashes can be in very large proportion and can precede the CG activity, it is necessary to take them into account to establish the general features of lightning activity in a given storm type [*Williams et al.*, 1999]. *Carey and Rutledge* [1998] studied a severe hailstorm by using data from multiparameter radar and electrical characteristics. They found an extremely high IC-to-CG ratio (up to 70) and predominantly positive CG flashes (over 74%). They noted strong values for the IC flash rate produced by this storm. Furthermore, the IC flash rate increased while the CG rate decreased or remained steady during the severe stage of the storm. In this case of severe thunderstorms, like in other cases studied by other authors [*MacGorman et al.*, 1989; *Maddox et al.*, 1997], both CG polarities stayed at low values for quite a long duration of their life cycles. Another study by *Lang et al.* [2000] examined in detail two intense convective storms observed during STERAO (Stratospheric-Tropospheric Experiment: Radiation, Aerosols and Ozone)-A in northeastern Colorado. Both storms studied showed very low CG flash rates ($<1$ min$^{-1}$) and, simultaneously, high IC flash rates ($>30$ min$^{-1}$) during part or all of their lifetimes. They also observed an anticorrelation between hail production and a significant rate of negative CG flashes. As indicated by many authors, the elevated charge mechanism could provide an interpretation for the high proportion of IC lightning flashes in severe storms, especially in those producing hail [*MacGorman et al.*, 1989]. In this theory, the strong updrafts loft all particles in the upper part of the cloud and limit the charge transfer between particles at a given level.

[5] This brief bibliographic review shows that the relation between the presence of hail in convective storms and the lightning activity is not clearly understood and documented. As indicated by *Williams* [2001] in a conclusion of its review on the topic, the examination of individual cases emphasizes a large variability. The goal of the present paper is first, to present some specific cases observed in European storms, and then, to discuss the relation between CG activity and hail in convective storms. Data were obtained during several campaigns and from several experimental tools. In each case, the presence of hail in the convective storms is detected with a specific method.

## 2. Data

[6] The observations used in the present study were made in three countries of southern Europe: France, Spain, and Italy. These three countries are equipped with CG lightning detection networks. The case of a thundercell occurring in northern Spain was covered by the French network and, therefore, the Spanish lightning data are not used in the study. For the French territory, for example, the network managed by the Météorage firm [*Tourte et al.*, 1988], is composed of 17 sensors of the Lightning Location and Protection (LLP) type, using the Direction Finder (DF) technique for lightning location. The performances of this network were improved in 1997 by combining the DF technique and the Time-Of-Arrival (TOA) technique for the location of the strokes. These new sensors are called IMPACT sensors. Location accuracy is thus better than 4 km for more than 70% of the strokes. More information about the detection and location combining DF technique and TOA technique can be found in *Cummins et al.* [1998]. The stations of the Italian network use also IMPACT sensors and the CG flashes were detected and located with an efficiency of more than 90% in northern Italy during the Mesoscale Alpine Program (MAP); [*Schulz*, 1997]. The data given by these networks allow the characterization of the CG activity with the following parameters: the location of the ground impact of each CG flash, its occurrence time, its polarity, its number of strokes (multiplicity), and the peak current of the strokes.

[7] Data for hail detection were issued from radar observations. Review about hail detection in convective storms by radar can be found in many papers [*Sauvageot*, 1992; *Kennedy et al.*, 2001; *Feral et al.*, 2003] and will not be discussed in detail here. Four approaches, that correspond to the four main methods of hail detection, are considered in section 3. Namely, (1) the value of the radar reflectivity factor (Z) at S band. For a carefully calibrated S-band radar, Z values larger than that corresponding to the highest possible rain rate (e.g., $>200$ mm h$^{-1}$) can be suspected to be associated with large hailstones. At short wavelength this approach is not possible because hailstones are non-Rayleigh scatterers [*Atlas and Ludlam*, 1961]. (2) The shape of the heavy precipitation reflectivity contours inside the convective storm: Characteristic shapes with overhang are associated with hailstorms [*Browning and Foote*, 1976]. (3) The polarimetric parameters: because hailstones are roughly spherical and raindrops are oblate spheroids, they are associated with significantly different values of polarimetric parameters [*Bringi et al.*, 1986; *Kennedy et al.*, 2001]. (4) The reflectivity difference of the hailfall for two radars working at C and S band: This difference appears because large hailstones are non-Rayleigh scatterers whose reflectivity depends on the wavelength [*Feral et al.*, 2003].

## 3. Case Studies

### 3.1. Hail Detection Based on the Reflectivity Value

[8] During the summer of 1996, a campaign of observations was made in southwestern France, at the Centre de Recherches Atmosphériques (CRA; Figure 1), in order to

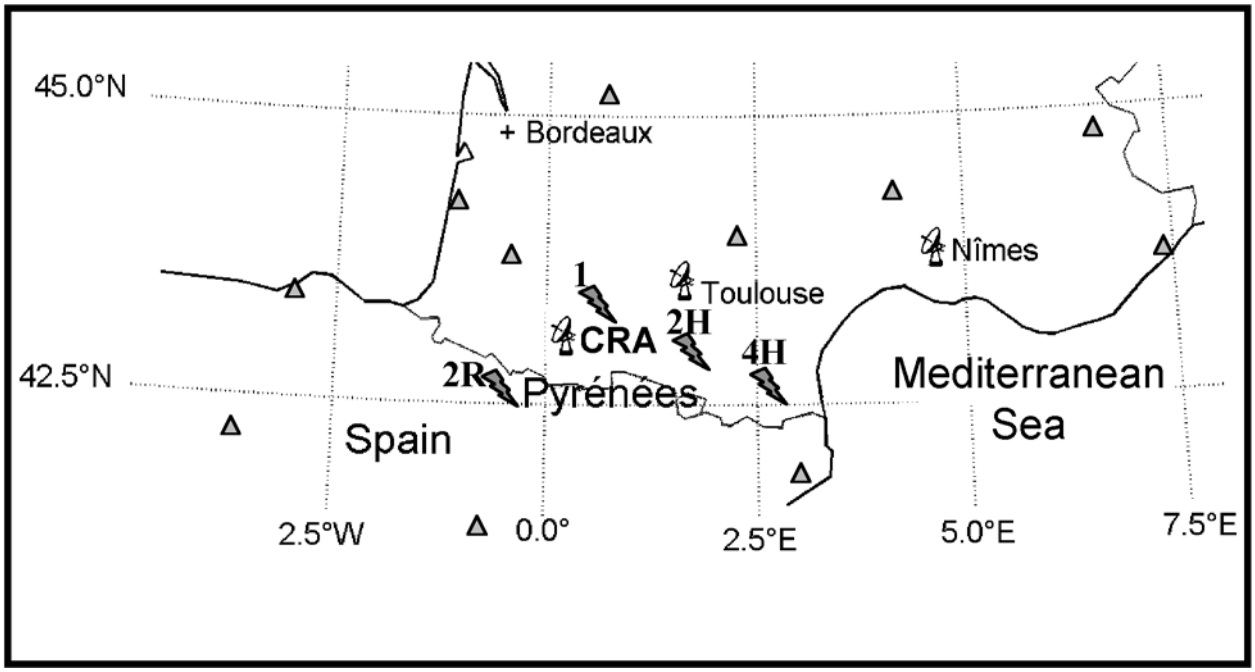


**Figure 1.** Map of the cases of convective storms occurring in southwestern France considered in this study. The radar and lightning flash symbols indicate the locations of the radar and of the different convective storms, respectively. The triangles indicate the locations of the CG detection stations.

study the correlation between several parameters of thunderstorms, especially the lightning activity and the thundercloud characteristics. For the cloud characteristics, the S-band radar of the Laboratoire d'Aérologie, located at the CRA (characteristics in Table 1) was used in Plan Position Indicator (PPI) and Range Height Indicator (RHI) modes. An example of observations from this radar was given in *Soula et al.* [1998] concerning a cell producing a flash flood in northern Spain on 7 August 1996.

[9] The case considered in this section was observed on 26 July 1996, when thundercells developed in the north and in the north-east of the CRA, at about 50 km. In Figure 1, the location of this thunderstorm activity is indicated with the lightning flash symbol labeled 1. Figure 2 displays two PPIs obtained with the radar at an elevation of 4.4° at 1753 UT for the first one (a) and at an elevation of 5° at 1811 UT for the second one (b). The domain represented is 100 × 100 km$^2$. The location of the radar corresponds to the site of the CRA at coordinates (0; 0) of the axes in the figure (43.13° N and 0.13° E in Figure 1). According to Figure 2, the horizontal distribution of the reflectivity factor Z in dBZ shows two well identified cells, 1R (Rain) and 1H (Hail), with values for Z reaching 40 and 45 dBZ at 1753 UT (at about 4 km of height) and 50 and 60 dBZ at 1811 UT (at about 5 km of height), respectively. Both cells were embedded in a cloud system with low radar reflectivity values at about 10 dBZ between 3 and 8 km of height. The locations of these cells did not vary very much from 1753 to 1811 UT, since they moved only a few kilometers in a northward direction. Their lifetimes were rather short (less than 1 hour) and they evolved quasi-synchronously. In the beginning, the reflectivity factors were slightly different, with the higher ones for Cell 1H. Then, the difference increased since at 1811 UT, they reached more than 60 dBZ in Cell 1H and only 50 dBZ in Cell 1R. Such values in Cell 1H could indicate a high probability of hail presence.

[10] Figure 2 also displays the CG flash locations, with minus and plus for negative and positive CG flashes, respectively. The flashes considered were produced during the 5 min surrounding the radar scans. Cell 1R produced many more CG flashes than Cell 1H, with a total of 309 during its whole lifetime compared to 36. Furthermore, the lightning production of Cell 1H was minimum around 1811 UT when the reflectivity factor was maximum. Figure 3a displays the evolution of the CG rates for both cells and for both CG polarities. Thus the rates of Cell 1R were higher with 34 in 5 min for negative CG flashes at 1755 UT and 38 in 5 min for all CG flashes at 1805 UT. These values were rather high for a short-lived thundercell. The positive and negative CG rates seem to be sometimes anticorrelated for Cell 1R. For Cell 1H, the CG rates were much lower, since the maximum values were 6, 2, 6 in 5 min for negative CG, positive CG, and total CG rates, respectively. Figure 3b displays the total CG flash density, including both polarities and calculated with a resolution of 5 × 5 km$^2$, in the whole area between 1730

**Table 1.** Characteristics of the Different Radars Used for the Observation of the Convective Storms Considered in the Study[a]

| Radar (section) | Wavelength, cm | Peak Power, kW | PRF, Hz | Beamwidth, deg | Type |
|---|---|---|---|---|---|
| CRA (3–1; 3–2) | 10.2 | 250 | 250 | 1.8 | - |
| Toulouse (3–4) | 5.3 | 250 | 330 | 1.3 | - |
| Nîmes (3–4) | 10.7 | 700 | 250 | 1.8 | - |
| Ronsard (3–3) | 5.3 | 250 | 1460 | 0.89 | D |
| MonteLema (3–3) | 5.5 | 250 | 600–1200 | 1 | D |
| S-Pol (3–3) | 10.3 | >1000 | 325–1200 | 0.91 | D-P |

[a]Section is related to the text of the present article (case studies). Type is D for Doppler, P for polarimetric.

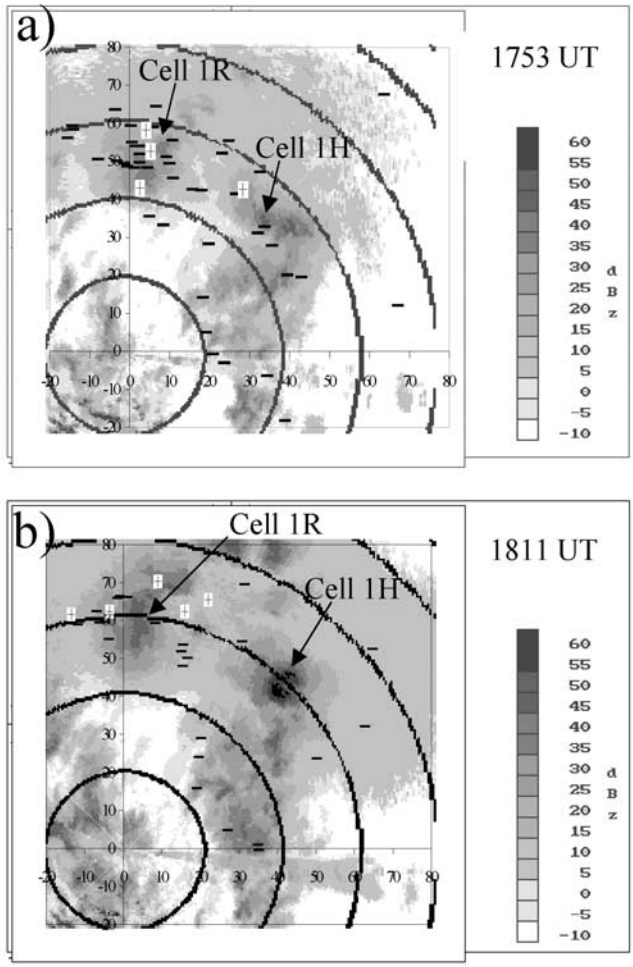


**Figure 2.** PPI radar display of the radar reflectivity factor Z (in dBZ) obtained from the S-band radar of the CRA at 1753 UT with an elevation of 4.4° (a) and at 1811 UT with an elevation of 5° (b) on 26 July 1996. The range markers are 20 km from each other and the arrows indicate the location of both hail-bearing (1H) and rain-producing (1R) cells. The axes are labeled in km and the CRA radar location is (0; 0). The CG flash strokes occurring during the 5 min surrounding the radar scans are located with the polarity indication (+ and −).

and 1830 UT. There again, a strong difference between both cells is pointed out. The maximum CG density was low, 0.68 $km^{-2}$ for Cell 1R, but its lifetime was rather short. The CG density calculated at this resolution can reach 2 $km^{-2}$ for a very active, stationary, thundercell with a long lifetime [*Soula et al.*, 1998] and it can easily exceed 1 $km^{-2}$ for a typical thundercell [*Soula and Chauzy*, 2001].

[11] Finally, all parameters relative to the CG flash activity (flash number, rate, and density) were much lower in the case of the thundercell providing larger reflectivity factor values. Typically, the ratios calculated for the flash density, the flash rate, and the flash number were 4.5, 7, and 8, respectively.

### 3.2. Hail Detection Based on the Radar-Echo Form

[12] During the same campaign of summer 1996, a thundercell was observed during the afternoon of 10 August. It is indicated by the lightning flash symbol labeled 2H in Figure 1 and was located 50 km east of the CRA at the beginning of its activity. This thundercell provided large reflectivities, with values exceeding 60 dBZ for 20 min and large volumes (several tens of $km^3$), as shown in Figure 4. This figure displays several RHIs made in the cell from 1337 to 1421 UT. They were made along an eastward direction in regard of the radar location and the thundercell moved following this direction with a velocity of about 60 km $h^{-1}$. The range marker circles in the figure are located 20 km from each other and the thundercell was between 40 and 50 km from the radar location at 1337 UT (Figure 4a). The horizontal dotted lines indicate the height above the ground 5 km by 5 km. In order to display the lightning activity evolution, the time series of the CG flash rate is represented in Figure 5, for 5-minute time intervals.

[13] At 1337 UT, the convective cell provided a radar reflectivity factor reaching 55 dBZ, a strong vertical development with a cloud top above 10 km, and a very low CG rate at only 2 in 5 min. The vertical development continued until 1400 UT to reach 15 km and the reflectivity values reached 60 dBZ between 5 and 10 km of height at about 1355 UT. Between 1355 and 1402 UT, the extent and height

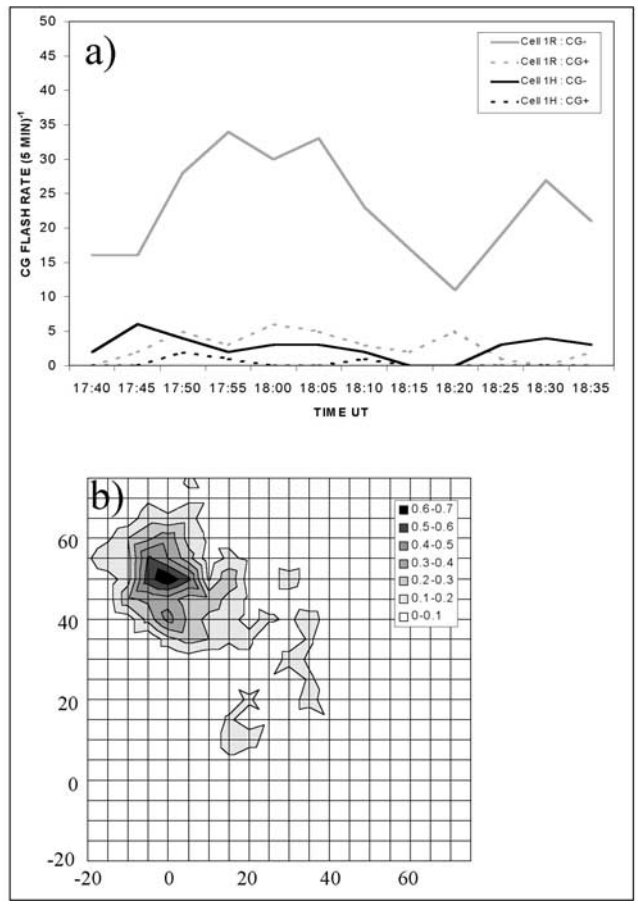


**Figure 3.** CG flash activity for both thundercells of 26 July 1996 during their lifetimes. (a) Evolution of the rates of the positive and negative CG flashes. (b) CG density in $km^{-2}$ averaged over 5 × 5 $km^2$. The axes are labeled in km and the CRA radar location is (0; 0). The grey levels represent the density in $km^{-2}$.

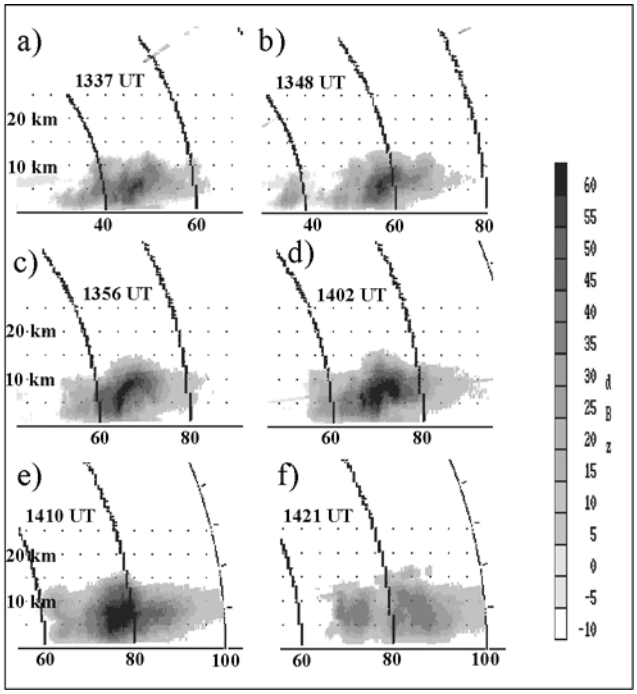


**Figure 4.** RHI radar displays of the radar reflectivity factor Z (in dBZ) obtained from the S-band radar of the CRA at 1337 UT (a), 1348 UT (b), 1356 UT (c), 1402 UT (d), 1410 UT (e), and 1421 UT (f) on 10 August 1996. The height level dotted lines and the circular range markers are 5 km and 20 km from each other, respectively. The radar is at an altitude of 600 m.

of the 60-dBZ reflectivity values increased while the corresponding vertical echo contour took the hook shape characteristic of a supercellular hailstorm [*Browning and Foote*, 1976]. On the other hand, after a substantial increase up to 9 flashes in 5 min at 1350 UT, the CG flash activity strongly decreased (Figure 5). Between 1410 and 1421 UT, the reflectivity abruptly decreased, since only 40 dBZ appeared in the 1421 UT scan. Ground observations revealed that, at the same time, large hailstones were falling in a small town (Daumazan, 09350), with a maximum hailstone diameter of about 39 mm for a duration of about 6 min around 1420 UT. This hailfall was responsible for the high radar reflectivity values observed aloft between 1356 and 1402 UT and it caused heavy damage to roofs, buildings, cars, and gardens in this town. Such characteristics allow to classify this thundercell as a severe storm and therefore the associated CG rates are really low for a storm of this type. After the hailfall, the CG flash rate increased to reach its maximum at 14 flashes during 1425–1430 UT.

[14] This rate can be compared with the CG flash rate of the thundercell causing a flash flood studied by *Soula et al.* [1998] and labeled in Figure 1 with the lightning flash symbol 2R. This thundercell had a very long lifetime and was especially stationary. Its CG flash rate reached up to 58 flashes in 5 min before progressively decreasing. Consequently, the CG flash density was large over the area of the thundercell development, more than 2 $km^{-2}$ in several $5 \times 5$ $km^2$ pixels [*Soula et al.*, 1998]. In the case of Cell 2H, the density calculated in the same conditions stayed below 0.3 $km^{-2}$. For the CG flashes produced during the lifetime and in the extent of the thundercell, the total number was about 1050 for Cell 2R studied by *Soula et al.* [1998], and only 73 for Cell 2H. There is clearly a strong contrast between the CG activities of the two cells. In terms of vertical development and horizontal extent, both thundercells were similar, except that the hail-bearing one exhibited larger reflectivity factors at the altitude of 7 km: 60 dBZ for Cell 2 H and only 45 dBZ for Cell 2R.

### 3.3. Hail Detection With a Polarimetric Radar

[15] During the Special Observation Period (SOP) of the Mesoscale Alpine Program (MAP), which occurred during autumn 1999 in northern Italy, a series of intensive observations was performed in cases of thunderstorms with several tools to characterize their dynamics, their microphysics, and their lightning activity [*Bougeault et al.*, 2001]. As indicated in Figure 6, a special instrumental coverage was performed over the Lago Maggiore Target Area (LMTA) including three Doppler radars (characteristics in Table 1): the French C-band Doppler radar Ronsard of the Centre d'étude des Environnements Terrestre et Planétaires (CETP), the operational Swiss C-band Doppler Monte-Lema radar of the Swiss Meteorological Agency (SMA), and the American S-band Doppler/Polarimetric S-Pol radar of the National Center for Atmospheric Research (NCAR). They covered the LMTA with a common observation area of about $140 \times 140$ $km^2$. The S-Pol radar could provide the microphysical structure of the convective system during its successive stages of development by using the particle-type identification algorithm described in *Vivekanandan et al.* [1999]. The input data of the algorithm are the polarimetric measurements (reflectivity factor Z, differential reflectivity ZDR, correlation coefficient at zero time lag $|\rho_{HV}|$, specific differential phase KDP, and linear depolarisation ratio LDR) and the temperature profile. By using this set of parameters and a fuzzy logic algorithm, the dominant particle type in terms of probability of presence is determined. The particles are classified into 11 types, including for example Heavy Rain (HR), Large Drops (LD), Hail (HL), Graupel/Hail mixture (GH). As indicated in section 2, the LMTA was covered by the Italian lightning detection network equipped with IMPACT stations. Furthermore, the networks from several neighboring countries were connected for the need

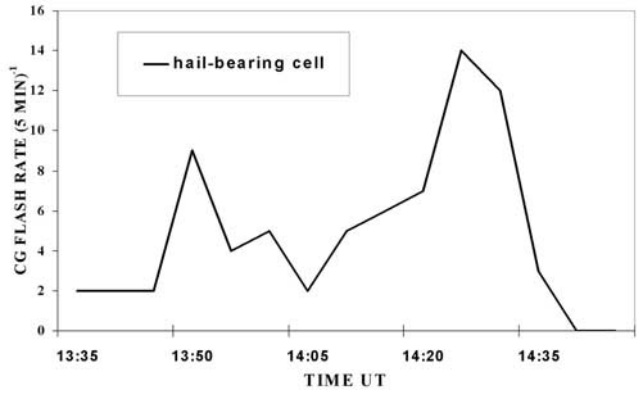


**Figure 5.** Evolution of the CG flash rate for the hail-bearing cell 2H observed on 10 August 1996. The rate is expressed in number of flashes per 5 min.

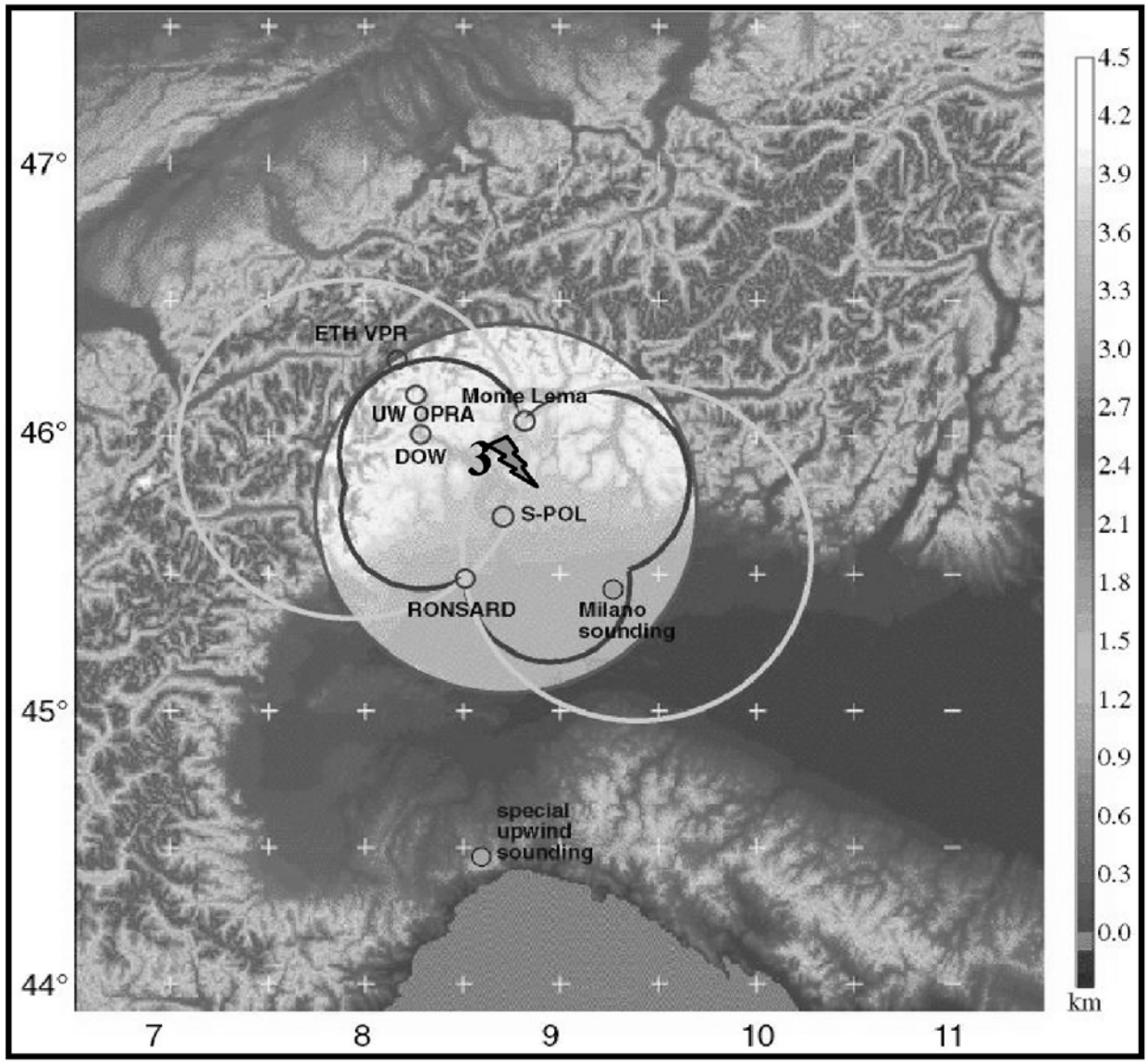


**Figure 6.** Map of the experimental study zone in the North of Italy. The Lago Maggiore Target Area (LMTA) is covered by circles representing the dual Doppler Ronsard/Monte-Lema area and that of S-Pol. The relief is described with a gray scale from 0 to 4.5 km. The flash symbol labeled 3 indicates the location of the cells considered in section 3.3. The horizontal and vertical scales of the surface indicate the longitude and the latitude in degree, respectively.

of the MAP experiment (France, Switzerland, Germany, Austria, and Italy).

[16] During the SOP, on 17 and 18 September, isolated cells and squall line-organized cells with high vertical developments crossed the LMTA. It was the most electrically active event during the MAP SOP: over an area of 250 × 250 km$^2$ centered near the S-Pol radar, 9880 CG flashes were detected between 1400 UT on 17 September and 0200 UT on 18 September [*Seity et al.*, 2003]. This intense convective activity was due to an eastward-moving trough combined with a convergence at low levels between two warm and moist air flows from the Adriatic Sea (easterly flow) and from Mediterranean Sea (southerly flow). The initial large-scale conditions, the dynamical and microphysical structure and evolution of this convective system were studied by *Richard et al.* [2003]. The lightning flash symbol with the label 3 in Figure 6 indicates the location of the thundercells considered in this study.

[17] In *Seity et al.* [2003], the radar data were used for the retrieval of the horizontal distributions of radar reflectivity and wind field at 1815 and 1830 UT on 17 September with a spatial resolution of 2.5 × 2.5 × 0.3 km$^3$. Two cells were active at that moment and their CG activity were quite different. One cell produced a total of 398 CG flashes, 5% of which were positive, and the other cell produced 342 CG flashes, 34% of which were positive. These cells are considered in the present study as Cells 3R and 3H, respectively. Figure 7 displays the distribution of the dominant particle types, at 1800 UT for the 3-km (a) and 6.9-km (b) levels, at 1815 UT for the 3-km (c) and 6.9-km (d) levels, and at 1830 UT for the 3-km (e) and 6.9-km (f) levels. In both cells and at both altitudes, the dominant

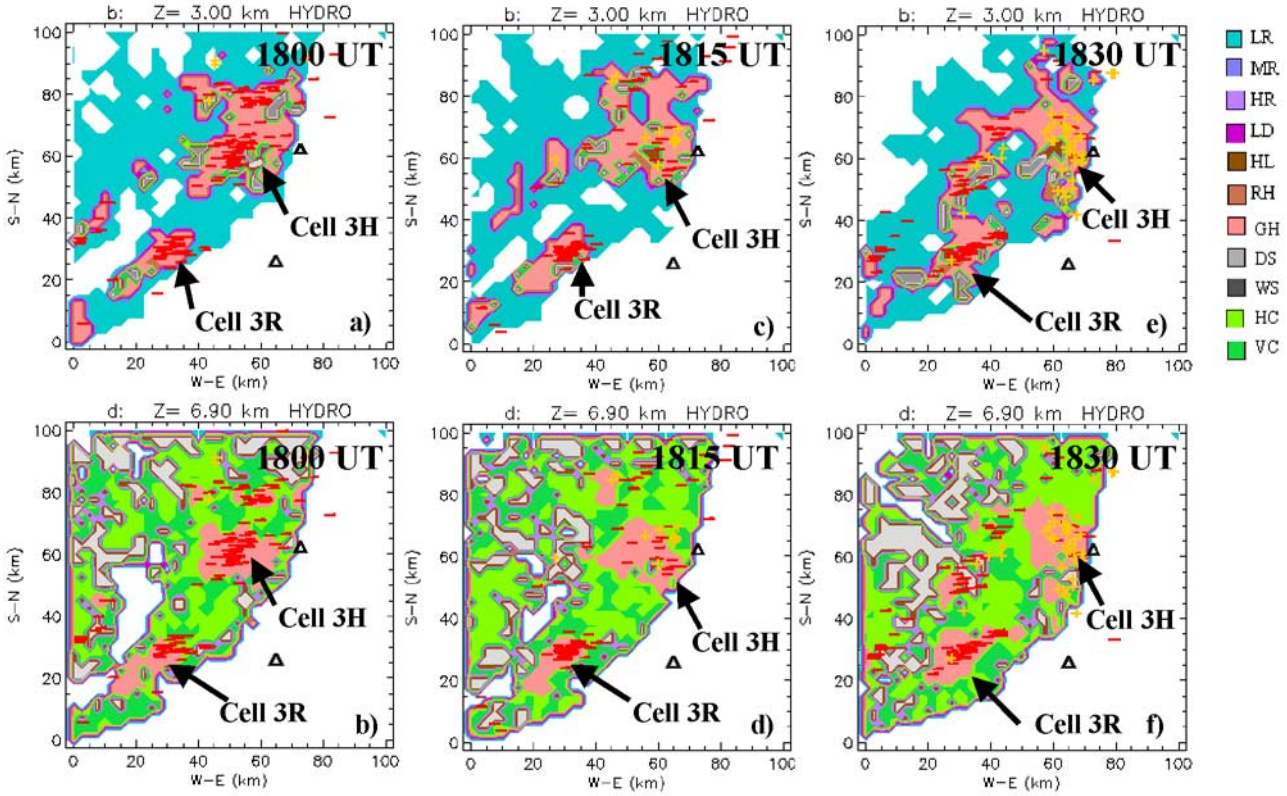


**Figure 7.** Horizontal cross sections of dominant hydrometeor type at altitudes 3 km (a, c, e), 6.9 km (b, d, f), at 1800 UT, 1815 UT, and 1830 UT, respectively, on 17 September 1999. (+) and (−) indicate the location of negative and positive CG flashes, respectively, occurring during the 15 min surrounding the cross section time. Both cells are indicated with an arrow.

type of particles was the mixture graupel/hail (GH) at 1800 UT. A strong correlation appears between the production of CG flashes and that of GH particles, especially at 6.9 km. At 1815 UT, the same correlation and the presence of hail in a large area of Cell 3H are visible. Cell 3H produced fewer CG flashes than at 1800 UT, which did not occur for Cell 3R. At 1830 UT Cell 3H produced a lot of positive CG flashes and hail was still visible at 3 km. In order to analyze the complete activity of both cells, the time series of their CG flash rates, hail volume, GH volume, and 35-dBZ echo top are displayed in Figure 8. For Cell 3R (Figure 8a), the time series were quite typical, exhibiting simultaneous increases of several parameters, for example the negative CG rate, the volume of the mixture Graupel-/Hail and the vertical velocity (not shown in Figure 8). The positive CG rate was appreciable at the end of the cell activity but with low values, 4 flashes in 5 min at the maximum at 1855 UT. On the contrary, Cell 3H exhibited a specific evolution with a large decrease of the negative CG rate at 1810 UT followed by a segment with dominant positive CG flashes (between 1815 and 1945 UT). During this segment, the negative CG rate was low, the hail and Graupel/Hail volumes were large. There again, the hail production seems to be associated with a low CG rate.

### 3.4. Hail Detection Using S- and C- Band Radar Reflectivity Difference

[18] On 21 April 1999, an eastward-moving convective cold frontal line swept southwestern France. At about 1700 UT, at the southern end of this line, a supercell hailstorm caused heavy damage, with hailstones up to 3–5 cm in diameter. The frontal line evolution, including the supercell hailstorm, was observed from birth to disappearance by two meteorological radars 200 km apart: the 5.3 cm radar located at Toulouse and the 10.7 cm radar located at Nîmes (Figure 1). The characteristics of both radars are given in Table 1. This storm was the most damaging over a period of about 10 years in the area of occurrence. This case is described in *Féral and Sauvageot* [2002] and *Féral et al.* [2003].

[19] From the almost synchronous observations of the rain field (i.e., at t ± 1 min) by each of the two radars, the hail areas were identified by computing the Dual-Wavelength Hail Ratio DWHR [*Féral et al.*, 2003]. This method uses the reflectivity difference of large hailstones between S- and C- band radars that is due to the non-Rayleigh scattering effects. The ratio of the relative reflectivity of the hail-suspected cell for the S-band radar to that for the C-band radar forms the dual-wavelength hail ratio DWHR:

$$\mathrm{DWHR} = \frac{\langle Z_{\mathrm{Hail}}^{10.7\mathrm{cm}} \rangle / \langle Z_{\mathrm{Rain}}^{10.7\mathrm{cm}} \rangle}{\langle Z_{\mathrm{Hail}}^{5.3\mathrm{cm}} \rangle / \langle Z_{\mathrm{Rain}}^{5.3\mathrm{cm}} \rangle} \quad (1)$$

From numerical simulations, *Féral et al.* [2003] found that the DWHR is linearly dependent on the difference between the azimuth widths O (O = d θ, where d is the

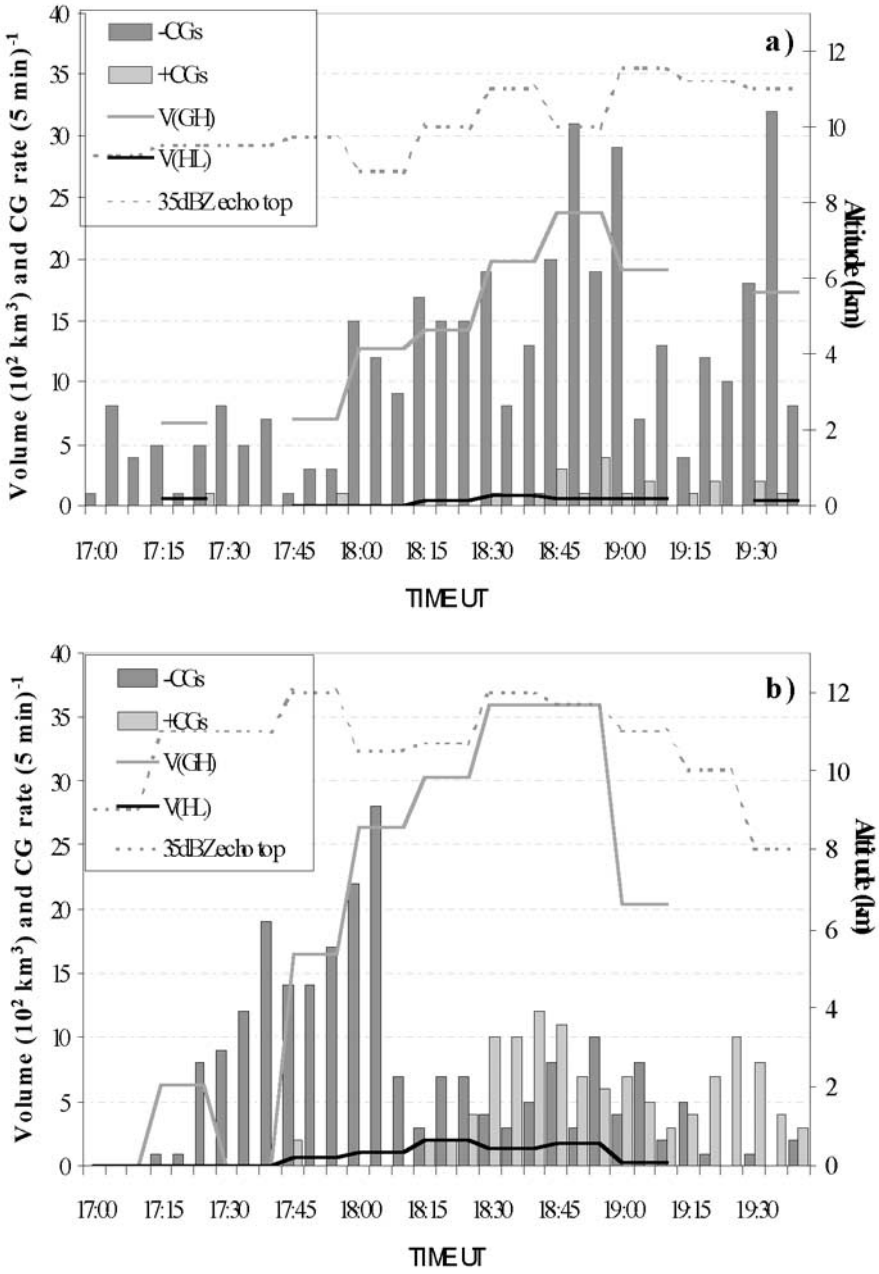


**Figure 8.** Time series of CG flash rates (+CG and −CG) estimated over 5-min intervals, of the volumes of the cloud with the hail dominant (V(HL)) and with the mixture hail-graupel dominant (V(GH)), and of the altitude of the 35-dBZ echo top for a) Cell 3R and b) Cell 3H.

radar-target distance and θ is the 3 dB beamwidth) of the S-band and C-band radars, that is, $(O_{10.7} - O_{5.3})$. Considering the characteristics of the radar of Toulouse and Nîmes, they defined an "equation of sensitivity" under the form: $DWHR = -0.0079 \times (O_{10.7} - O_{5.3}) + 1.05$. For cells producing liquid precipitation only, $DWHR \leq -0.0079 \times (O_{10.7} - O_{5.3}) + 1.05$, while in the presence of hailstones greater than about 2.5 cm in diameter (i.e., non-Rayleigh scatterers), $DWHR > -0.0079 \times (O_{10.7} - O_{5.3}) + 1.05$.

[20] Figure 9a shows the evolution of the DWHR computed for the 21 April 1999 supercell hailstorm from 1700 to 1840 UT. This evolution displays a signal characteristics of a hailstorm. In the studied area, no other DWHR signal of hail was detected for that day. According to Figure 9a, the hailstorm exhibited three hail events with hailstones greater than 2.5 cm in diameter. The first one occurred between 1705 and 1720 UT, the second one between 1725 and 1800 UT, and the third one between 1819 and 1827 UT. The second one lasted 35 min and exhibited the DWHR maximum value of 115% toward 1740 UT. The three hail production periods coincided with the evolution of the supercell hailstorm, from its birth at around 1700 UT to its disappearance at about 1835 UT. The reflectivity factor exceeded 60 dBZ at 2 km of height for several tens of min

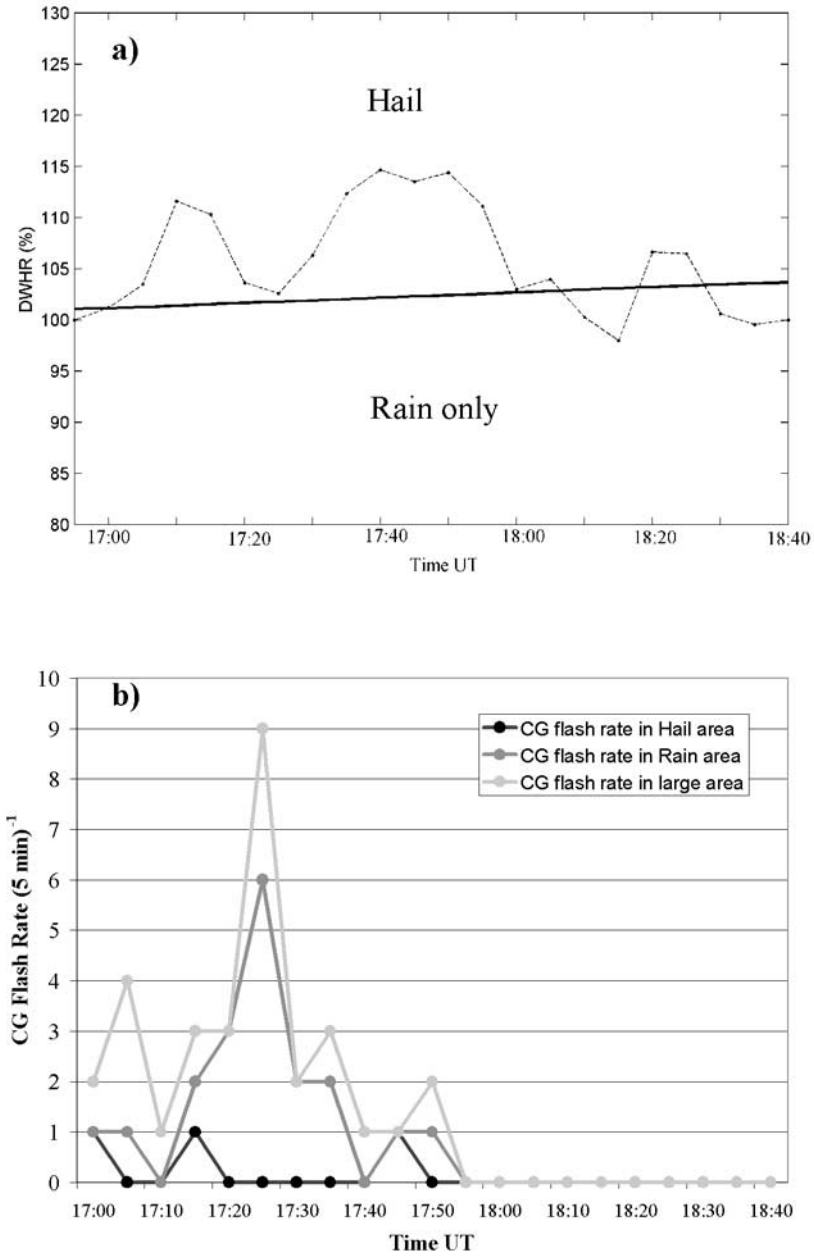


**Figure 9.** (a) Supercell dual-wavelength reflectivity hail ratio (DWHR) variation from 1700 UT to 1840 UT on 21 April 1999. Every point corresponds to DWHR computed from simultaneous observations of the supercell by the radars of Toulouse and Nîmes every 5 min. The bold line stands for the sensitivity equation DWHR = $-0.0079 \times (O_{10.7} - O_{5.3}) + 1.05$ established from simulations for the French radar network (adapted from *Féral et al.*, 2003). (b) Evolution of the CG flash rate calculated over 5-min intervals for several areas of the supercell, namely the hail area, the rain area, and an area extended by 5 km around the rain area.

[*Feral et al.*, 2003]. MétéoFrance (the French national weather organization) indicated hail falls only on the zone swept by the supercell. No other occurrence of hail was observed at the ground in the other parts of the convective field.

[21] The CG rate during this event was evaluated in several areas as indicated in Figure 9b. The first area corresponds to that where hail was detected, the second one corresponds to that where rain or hail was detected, and the third one corresponds to the second one extended by 5 km around. All CG rates were low, especially that in the first area. Those of second and third areas exhibited maximums at 1725 UT (9 flashes in 5 min for a 30 $\times$ 28 km$^2$ area) and stayed at zero after 1800 UT whereas the radar echoes were still strong. Therefore the CG production was low when a strong probability of hail presence was

indicated by the large values of DWHR between 1730 and 1800 UT.

## 4. Discussion

[22] All the cases considered in this study clearly show a low CG flash production when hail is probably present in the thundercloud and even when the severe character of the cell is formally established. The comparison of the CG activity of the hail-bearing cells with that of the others thundercells considered or with other works justifies this remark. For these hail-bearing cells, the CG rate did not exceed 2 $min^{-1}$ which also was considered as a low rate by *Lang et al.* [2000]. The CG rate can peak at about 12 $min^{-1}$ in supercells as indicated by *Soula et al.* [1998] or *Williams et al.* [1999], and even up to 20 $min^{-1}$ according to *Knapp* [1994]. Two kinds of CG activity evolution were observed: one with a low rate throughout the thundercell lifetime as for Cell 2H (section 3.2); the other with a large decrease in the CG rate corresponding to the hail production, like for Cell 3H (section 3.3). In the second case, simultaneously to the CG flash rate decrease, an increase in the positive CG proportion was observed. If the CG rate was low even though the cloud development and the radar reflectivity factor are strong, several interpretations may be put forth. Other studies have shown enhanced intracloud/cloud-to-ground ratios during the severe stage of storms [*MacGorman et al.*, 1989; *Carey and Rutledge*, 1998]. On the contrary, no observation has displayed a low total flash rate from hail-producing storms.

[23] First, if the CG activity is weak, the elevated charge mechanism model could explain this feature. Thus in this hypothesis, as explained by *MacGorman et al.* [1989], the strong updrafts can have several consequences on the CG activity by directly affecting the non-inductive processes or by lofting the charged particles in the upper part of the cloud. The strong updrafts could limit the time during which particles stay at a given level where they grow and acquire charge, or they could enhance the temperature at a given level and cause the increase in the height of the non-inductive ice process. In this case of explanation, the observation of the IC lightning activity is necessary to confirm it. In the present study, no information was obtained about the total lightning activity. The study by *Lang et al.* [2000] analyzed two cases of hailstorms documented in total lightning activity. Both cases exhibited a common feature with the present cases: When the hail was produced, the CG flash rate was low. Another observation made by *Lang et al.* was that when the cells were strongly developed, the IC flash rates were high. They concluded that their observations were consistent with the elevated charge hypothesis. However, they observed another feature common to their hailstorms, the CG rates remained low even during the storm collapsing in contrast to the typical observation made on the evolution of the lightning activity during the storm lifetime [*Williams et al.*, 1989]. Our hailstorms cases seem to correspond also to this feature since their CG rates are low all the time. Furthermore, in one case (Cell 3H), the positive CG proportion is very high during the second phase of the cell lifetime and the corresponding rate is especially high compared with typical values in common thunderstorms. The elevated dipole theory cannot explain why the positive CGs are enhanced and the negative ones are reduced.

**Table 2.** Characteristics of the +CG and −CG Flashes Produced by the Thundercells Considered in the Study[a]

| | | −CG | | | +CG | | |
|---|---|---|---|---|---|---|---|
| Date of Event | Domain | N | $I_{MAX}$, kA | M | N | $I_{MAX}$, kA | M |
| 26 July 1996 | Area | 1547 | −35.6 | 2.13 | 290 | 56.9 | 1.08 |
| | Cell 1R | 275 | −29.8 | 2.21 | 34 | 30.0 | 1.07 |
| | Cell 1H | 32 | −31.7 | 1.98 | 4 | 40.2 | 1.10 |
| 7 August 1996 | Area | 4232 | −32.8 | 2.34 | 190 | 40.2 | 1.21 |
| | Cell 2R | 1011 | −33.2 | 2.63 | 39 | 41.2 | 1.05 |
| 10 August 1996 | Area | 3980 | −34.3 | 1.91 | 66 | 49.9 | 1.03 |
| | Cell 2H | 72 | −36.3 | 2.10 | 1 | 51.7 | 1.00 |
| MAP 17 Sept. 1999 | Area | 9836 | −19.8 | 2.42 | 1462 | 26.6 | 1.41 |
| | Cell 3R | 377 | −20.0 | 2.34 | 21 | 16.1 | 1.05 |
| | Cell 3Ha | 152 | −17.7 | 1.98 | 2 | 11.2 | 1.00 |
| | Cell 3Hb | 73 | −12.5 | 1.16 | 115 | 33.5 | 1.13 |
| 21 April 1999 | Area | 325 | −24.4 | 1.75 | 22 | 35.2 | 1.00 |
| | Cell 4H | 20 | −20.9 | 1.80 | 0 | - | - |

[a]The number of flash N, the peak current $I_{MAX}$, the multiplicity M. For each event, Area represents the domain of the study.

[24] Another type of interpretation for the weak lightning activity could concern the lightning initiation conditions. As a matter of fact, according to some results of model studies, the iced particles could be less favorable to the triggering off of lightning than liquid particles because of a weaker enhancement of the electric field [*Coquillat and Chauzy*, 1994]. The falling water drops can acquire an elongated shape, whereas the iced particles are rigid. A supplemental element can be considered in our case, the characteristics of the CG flashes produced by the different cells, especially those relative to the charge neutralized: The peak current and the multiplicity of the CG flashes are available for all events studied. As a matter of fact, in winter storms where the triggering conditions could be worse, the charge neutralized by the ground flashes is generally higher [*Brook*, 1992]. Table 2 thus displays the different characteristics of the CG flashes produced by these thundercells.

[25] Previous studies gave the average values and the main features of variability for both peak current and multiplicity and for both CG flash polarities. For the negative CG flashes, the average peak current was then found between −20 and −30 kA and the average multiplicity was found between 1.6 and 3.1 according to *Berger et al.* [1975] and *Sheridan et al.* [1997]. The variability of these parameters is linked to several factors, especially the latitude, the season, and the climatic conditions. The sensitivity of the network also could have an influence about these parameters and it is important to be careful in the comparison of data from different networks. According to a recent study by *Orville et al.* [2002] on the North American continent and over an entire period of three years, the median negative peak current and the negative multiplicity largely depend on the location. Furthermore, both are correlated since the higher the negative multiplicity, the higher the median negative peak current. Thus the median negative peak current is high (>20 kA in absolute value) along the coasts and in the South (Oklahoma, Florida, etc.) where the activity is quite high. It is important to note that the median value can be lower than the mean value for this current because of some very large values. For the positive

CG flashes, the peak current is generally higher with average values exceeding 35 kA in some part of the United States [*Orville et al.*, 2002], between 50 and 100 kA for averaged values over shorter periods and over small areas [*Sheridan et al.*, 1997] in the South-Central United States. The multiplicity is lower for this CG flash polarity since *Sheridan et al.* [1997] found between 1.37 and 2. In the study by *Orville et al.* [2002], the variability of these parameters is large at continental scale. In this case, the median positive current decreased with the multiplicity. In most of the North American continent the positive multiplicity is lower than 1.2 and the median positive peak current can locally exceed 35 kA when the proportion of positive CG flashes is high. In the regions with a low percentage of positive CG flashes, the median positive peak current is low (<20 kA).

[26] By considering the characteristics reported in Table 2, we note a difference between the 1996 summer cases in southwestern France and the other cases of April 1999 and September 1999. For the first cases, the mean peak currents are close from one cell to another, with values around −30 kA for the negative ones and 40−50 kA for the positive ones. These values are typical compared to other studies. The multiplicity also was typical and quite constant from a case to another, with values from 1.9 to 2.6 for the negative CG flashes and from 1.0 to 1.2 for the positive ones. In the other cases, the peak currents were lower, especially for the negative CG flashes. For example in Cell 3H of MAP, the mean peak current was −17.7 kA during the first phase of its activity (cell 3Ha in Table 2) and −12.5 kA during the second phase (cell 3Hb in Table 2) when the positive CG flashes were dominant (Figure 7). Furthermore, during this second phase, the negative multiplicity was very low at 1.16. On the contrary, the corresponding positive peak current was high at 33.5 kA compared to the first phase where it was only 11.2 kA. In this case of hail-bearing cell (Cell 3H of MAP), the values of peak current and multiplicity show that the negative charge available in the cloud was low during the hail-production period. It is not consistent with the explanation including worse triggering conditions which would involve large peak currents when the flash rates were low.

[27] If the main mechanisms for explaining the electrification of thunderclouds are the non-inductive processes [*Saunders*, 1993], the explanation of a low charge production has to be found in the presence of hail in the particle collisions. In the presence of large hailstones in the cloud, the number of collisions with ice crystal could be lower and therefore the charge exchanged in the cloud could be reduced. According to *Keith and Saunders* [1990], the charge per collision between ice crystal and ice particle (hailstone, graupel) increases with the size of the ice crystal but the increase rate is lower for large particles. Therefore the increase of the charge transferred in the collision with the size of ice particle could not compensate the decrease of the total charge transferred, due to a lower number of collision in the case of large particles. According to different authors, many parameters can govern the polarity and the charge amount transferred when particles collide. For example *Jayaratne and Saunders* [1985] demonstrated that charging depended on liquid droplets colliding with the graupel. The proportion of liquid water colliding with the graupel depends on the aerodynamic forces [*Saunders et al.*, 1991]. Of course, it is difficult to give more detail about this aspect of interpretation because collection efficiencies for water droplets are quite complex and depend on the size of both the collector and collected particles.

[28] As observed in the case of Cell 3H, the production of hail is associated with strong vertical wind velocities. Other works discussed relationships between ground lightning activity and severe weather. However, the number of studies with extensive data on both ground lightning flash polarities and storm evolution is still small. For example, *Reap and MacGorman* [1989], found that the probability of severe weather slightly increased for storms producing larger numbers of ground flashes up to 130 flashes per grid box ($48 \times 48$ km$^2$) and then decreased as the number of ground flashes further increased. On the contrary, if they distinguished the time evolution of both polarities of ground flashes, this probability increased very quickly with the number of positive ground flashes, even for large numbers. Therefore the high proportion of positive ground flashes can be an indicator of severe weather and therefore of hail production. Several works reported cases of severe weather associated with large concentrations of positive CG flashes [*Branick and Doswell*, 1992; *Seimon*, 1993; *MacGorman and Burgess*, 1994]. Several hypothesis to interpret this observation are summarized by *Williams* [2001]. Among the cases of hail-bearing cells considered here, only one produced a high proportion and high density of positive ground flashes (Cell 3H). The other cells produced very low ground flash rates of both polarities. The intensity of the negative ground flashes is very low in the case of a high positive ground flash proportion. When the positive ground flashes are produced by Cell 3H, they are located at the edge of the high reflectivity core of the cell and around the hail location (Figure 7). According to other authors, in the case of intense positive ground flash activity, the positive strike points can be observed around the high reflectivity core [*Carey and Rutledge*, 1998] or throughout the high-reflectivity region [*Seimon*, 1993]. Recent works [*Williams et al.*, 1999] show also that the total lightning activity tends to lead severe weather on the ground. This information would be really necessary to better understand the general relation between cloud physics and lightning activity.

## 5. Conclusion

[29] Thunderstorm observations collected simultaneously by radar and CG flash detection devices allowed us to point out a specific lightning flash activity associated with the hail-bearing thundercells. The presence of hail is deduced from different techniques according to the type of radar data available. So, the radar reflectivity factor value, the radar echo form, the polarimetric radar data treatment, and the dual wavelength radar data are successively used for this aim. All thunderstorms in this study occurred in southwestern France or northern Italy.

[30] A common feature is low-CG production by hail-bearing thundercells. While the CG rate for a very active thundercell can easily reach more than 10 min$^{-1}$, in the cases of strong thundercells presented here this rate did not exceed 2 min$^{-1}$ when the cells produced hail during their lifetime. Some of these thundercells displayed these low flash rates

throughout their lifetime, whereas one other exhibited a strong decrease of this rate and a change of the dominant polarity of the CG flashes from negative to positive. In these cases, after this polarity change, the negative CG flashes exhibited very low peak current and multiplicity.

[31] To explain the low rate of CG flashes, three interpretations are discussed: the first one is related to the elevated charge dipole, the second one is related to the triggering conditions, and the third one related to the charge transfer. The first one has been discussed in other works and the data available in this study do not allow a new evaluation of this theory. However, some observations with large positive CG proportions during the hailstorm activity cannot be explained with this theory. In the second one, the CG flash could exhibit large peak current and multiplicity, as it is the case in winter storms [*Brook*, 1992]. The observations tend to show typical values and sometimes low values for both parameters, therefore this hypothesis stays few probable. The discussion about the interpretation related to the charge transfer conditions is more developed.

[32] Several ideas are proposed to explain the low CG flash rate associated with hail, by considering the non-inductive charging process. The main interpretations call for a low number of collisions due to particle size in the case of hail, a low efficiency in charge transfer between large particles, and a significant number of non-rebounding collisions. In all the cases considered, no information about the intracloud lightning activity was available and therefore it is difficult to conclude about the global charge transfer when hail is largely present in the cloud. Such information would be useful to reach a better interpretation of the present observations.

[33] **Acknowledgments.** The authors are grateful to MétéoFrance, the French national weather organization, for providing the data for the case of 21 April 1999. They are grateful to the ALDIS Society for providing CG data collected during the MAP campaign, and to the teams of the S-Pol radar and of the Ronsard radar working on this campaign. They thank Michel Chong and Jean-François Georgis from the Laboratoire d'Aérologie for their technical help on Doppler and polarimetric radar data processing. The authors thanks also the three anonymous reviewers for valuable comments and suggestions.

## References

Atlas, D., and F. H. Ludlam (1961), Multi-wavelength radar reflectivity of hailstorms, *Q. J. R. Meteorol. Soc.*, *87*, 523–534.

Baughman, R. G., and D. M. Fuquay (1970), Hail and lightning occurrence in mountain thunderstorms, *J. Appl. Meteorol.*, *9*, 657–660.

Berger, K., R. B. Anderson, and H. Kröninger (1975), Parameters of lightning flashes, *Electra*, *41*, 23–37.

Blevins, L. L., and J. D. Marwitz (1968), Visual observations of lightning in some Great Plains hailstorms, *Weather*, *23*, 192–194.

Bougeault, P., P. Binder, A. Buzzi, R. Dirks, R. Houze, J. Kuettner, R. B. Smith, R. Steinacker, H. Volkert, and MAP scientists (2001), The MAP special observing period., *Bull. Am. Meteorol. Soc.*, *82*, 433–462.

Branick, M. L., and C. A. Doswell III (1992), An observation of the relationship between supercell structure and lightning ground strike polarity, *Weather Forecast.*, *7*, 143–149.

Bringi, V. N., J. Vivekanandan, and J. D. Tuttle (1986), Multiparameter radar measurements in Colorado convective storms. Part II: Hail detection studies, *J. Atmos. Sci.*, *43*, 2564–2577.

Brook, M. (1992), Breakdown electric fields in winter storms, *Res. Lett. Atmos. Electr.*, *12*, 47–52.

Browning, K. A., and C. B. Foote (1976), Airflow and hail growth in supercell storms and some implications for hail suppression, *Q. J. R. Meteorol. Soc.*, *102*, 499–534.

Carey, L. D., and S. A. Rutledge (1998), Electrical and multiparameter radar observations of a severe hailstorm, *J. Geophys. Res.*, *103*, 13,979–14,000.

Changnon, S. A. (1992), Temporal and spatial relations between hail and lightning, *J. Appl. Meteorol.*, *31*, 587–604.

Coquillat, S., and S. Chauzy (1994), Computed conditions of corona emission from raindrops, *J. Geophys. Res.*, *99*, 16,897–16,905.

Cummins, K. L., M. J. Murphy, E. A. Bardo, W. L. Hiscox, R. B. Pyle, and A. E. Pifer (1998), NLDN'95: A combined TOA/MDF technology upgrade of the US National Lightning Detection Network, *J. Geophys. Res.*, *103*, 9035–9044.

Engholm, C. D., E. R. Williams, and R. M. Dole (1990), Meteorological and electrical conditions associated with positive cloud-to-ground lightning, *Mon. Weather Rev.*, *118*, 470–487.

Féral, L., and H. Sauvageot (2002), Fractal identification of supercell storms, *Geophys. Res. Lett.*, *29*(14), doi:10.1029/2002GL015260.

Féral, L., H. Sauvageot, and S. Soula (2003), Hail detection using S- and C- band radar reflectivity difference, *J. Atmos. Oceanic Technol.*, *20*, 233–248.

Fuquay, D. M. (1982), Positive cloud-to-ground lightning in summer thunderstorms, *J. Geophys. Res.*, *87*, 7131–7140.

Holle, R. L., and M. W. Maier (1982), Radar echo height related to cloud-to-ground lightning in South Florida, *12th Conference On Severe Storms*, pp. 330–333, Am. Meteorol. Soc., San Antonio, Tx.

Jayaratne, E. R., and C. P. R. Saunders (1985), Thunderstorm electrification: The effect of cloud droplets, *J. Geophys. Res.*, *90*, 13,063–13,066.

Keith, W. D., and C. P. R. Saunders (1990), Further laboratory studies of the charging of graupel during ice crystal interactions, *Atmos. Res.*, *25*, 445–464.

Kennedy, P. C., A. Rutledge, W. A. Petersen, and V. N. Bringi (2001), Polarimetric radar observations of hail formation, *J. Appl. Meteorol.*, *40*, 1347–1366.

Knapp, D. I. (1994), Using cloud-to-ground lightning data to identify tornadic thunderstorm signatures and nowcast severe weather, *Natl. Wea. Dig.*, *19*, 35–42.

Lang, T. J., S. A. Rutledge, J. E. Dye, M. Venticinque, P. Laroche, and E. Defer (2000), Anomalously low negative Cloud-to-Ground lightning flash rates in intense convective storms observed during STERAO-A, *Mon. Weather Rev.*, *128*, 160–173.

MacGorman, D. R., and D. W. Burgess (1994), Positive cloud-to-ground lightning in tornadic storms and hailstorms, *Mon. Weather Rev.*, *122*, 1671–1697.

MacGorman, D. R., D. W. Burgess, V. Mazur, W. D. Rust, W. L. Taylor, and B. C. Johnson (1989), Lightning rates relative to tornadic storm evolution on 22 May 1981, *J. Atmos. Sci.*, *46*, 221–250.

Maddox, R. A., K. W. Howard, and C. L. Dempsey (1997), Intense convective storms with little or no lightning over central Arizona: A case of inadvertent weather modification?, *J. Appl. Meteorol.*, *36*, 302–314.

Orville, R. E., G. R. Huffines, W. R. Burrows, R. L. Holle, and K. Cummins (2002), The North American Lightning Detection Network (NALDN)-First results: 1998–2000, *Mon. Weather Rev.*, *130*, 2098–2109.

Pakiam, J. E., and J. Maybank (1975), The electrical characteristics of some severe hailstorms in Alberta, *Canada. J. Meteorol. Soc. Jpn.*, *53*, 363–383.

Reap, R. M., and D. R. MacGorman (1989), Cloud-to-Ground lightning: Climatological characteristics and relationships to model fields, radar observations, and severe local storms, *Mon. Weather Rev.*, *117*, 518–535.

Richard, E., S. Cosma, P. Tabary, J. P. Pinty, and M. Hagen (2003), High-resolution numerical simulations of the convective system observed in the Lago Maggiore area on 17 September 1999(MAP IOP 2a), *Q. J. R. Meteorol. Soc., 129*, *588*, 543–563.

Rust, W. D., W. L. Taylor, D. R. MacGorman, and R. T. Arnold (1981), Research on electrical properties of severe thunderstorms in the Great Plains, *Bull. Am. Meteorol. Soc.*, *62*, 1286–1293.

Rutledge, S. A., and D. R. MacGorman (1988), Cloud-to-ground lightning activity in the 10–11 June 1985 Mesoscale Convective System observed during the Oklahoma-Kansas PRE-STORM project, *Mon. Weather Rev.*, *116*, 1393–1408.

Saunders, C. P. R. (1993), A review of thunderstorm electrification processes, *J. Appl. Meteorol.*, *32*, 642–655.

Saunders, C. P. R., W. D. Keith, and R. P. Mitzeva (1991), The effect of liquid water on thunderstorm charging, *J. Geophys. Res.*, *96*, 11,007–11,017.

Sauvageot, H. (1992), *Radar Meteorology*, Artech House, 366 pp., Washington, D. C.

Schulz, W. (1997), Performance evaluation of lightning location systems, Ph.D. thesis, Tech. Univ. of Vienna, Vienna, Austria.

Seimon, A. (1993), Anomalous cloud-to-ground lightning in a F5-tornado-producing supercell thunderstorm on 28 August 1990, *Bull. Am. Meteorol. Soc.*, *74*, 189–203.

Seity, Y., S. Soula, P. Tabary, and G. Scialom (2003), The convective storm system during IOP 2a of MAP: Cloud-to-ground lightning flash production in relation to dynamics and microphysics, *Q. J. R. Meteorol. Soc., 129*, *588*, 523–542.

Shackford, C. R. (1960), Radar indications of a precipitation-lightning relationship in New England thunderstorms, *J. Meteorol.*, *17*, 15–19.

Sheridan, S. C., J. H. Griffits, and R. E. Orville (1997), Warm season cloud-to-ground lightning-precipitation relationships in the South-Central united States, *Weather Forecast.*, *12*, 449–458.

Soula, S., and S. Chauzy (2001), Some aspects of the correlation between lightning and rain activities in severe storms, *Atmos. Res.*, *56*, 355–373.

Soula, S., H. Sauvageot, G. Molinié, F. Mesnard, and S. Chauzy (1998), The CG lightning activity of a storm causing a flash-flood, *Geophys. Res. Lett.*, *25*(8), 1181–1184.

Stolzenburg, M. (1994), Observations of high ground flash densities of positive lightning in summertime thunderstorms, *Mon. Weather Rev.*, *122*, 1740–1750.

Tourte, J. L., F. Helloco, M. Le Boulch, and J. Hamelin (1988), First results obtained with the Météorage thunderstorm monitoring system, in *Proceedings of the 8th Conference on Atmospheric Electricity*, pp. 697–702, Inst. of High Voltage Res., Uppsala, Sweden.

Vivekanandan, J., D. S. Zrnic, S. M. Ellis, R. Oye, A. V. Rhyzhkov, and J. Straka (1999), Cloud Microphysics retrieval using S-Band dual-polarization radar measurements, *Bull. Am. Meteorol. Soc.*, *80*, 381–388.

Williams, E. R. (2001), The electrification of severe storms, *Meteorol. Monogr.*, *28*, 527–561.

Williams, E. R., M. E. Weber, and R. E. Orville (1989), The relationship between lightning type and convective state of thunderclouds, *J. Geophys. Res.*, *94*, 13,213–13,220.

Williams, E. R., et al. (1999), The behavior of total lightning activity in severe Florida thunderstorms, *Atmos. Res.*, *51*, 245–264.

L. Feral, Département Electromagnétisme et Radar, Office National d'Etudes et de Recherches Aérospatiales-Centre de Toulouse, F-31055 Toulouse, France.

H. Sauvageot and S. Soula, Laboratoire d'Aérologie, UMR 5560 UPS/CNRS, OMP, 14 avenue Edouard Belin, F-31400 Toulouse, France. (sous@aero.obs-mip.fr)

Y. Seity, Météo-France, F-31057 Toulouse, France.